PCCP

PAPER

View Article Online
View Journal | View Issue

Cite this: *Phys. Chem. Chem. Phys.*, 2017, **19**, 11968

DFT-D3 study of H_2 and N_2 chemisorption over cobalt promoted Ta_3N_5-(100), (010) and (001) surfaces

Constantinos D. Zeinalipour-Yazdi,[a] Justin S. J. Hargreaves,[b] Said Laassiri[b] and C. Richard A. Catlow*[ac]

The reactants for ammonia synthesis have been studied, employing density functional theory (DFT), with respect to their adsorption on tantalum nitride surfaces. The adsorption of nitrogen was found to be mostly molecular and non-activated with side-on, end-on and tilt configurations. At bridging nitrogen sites (Ta–N–Ta) it results in an azide functional group formation with a formation energy of 205 kJ mol^{-1}. H_2 was found also to chemisorb molecularly with an adsorption energy in the range −81 to −91 kJ mol^{-1}. At bridging nitrogen sites it adsorbs dissociatively forming >NH groups with an exothermic formation energy of −175 kJ mol^{-1} per H_2. The nitrogen vacancy formation energies were relatively high compared to other metal nitrides found to be 2.89 eV, 2.32 eV and 1.95 eV for plain, surface co-adsorbed cobalt and sub-surface co-adsorbed cobalt Ta_3N_5-(010). Co-adsorption of cobalt was found to occur mostly at nitrogen rich sites of the surface with an adsorption energy that ranged between −200 to −400 kJ mol^{-1}. The co-adsorption of cobalt was found to enhance the dissociation of molecular hydrogen on the surface of Ta_3N_5. The studies offer significant new insight with respect to the chemistry of N_2 and H_2 with tantalum nitride surfaces in the presence of cobalt promoters.

Received 6th February 2017,
Accepted 6th April 2017

DOI: 10.1039/c7cp00806f

rsc.li/pccp

1. Introduction

Understanding the mechanism of catalytic reactions is critical in the development of new catalyst formulations and process conditions that have lower energy requirements. In catalytic reactions, the role of defects and promoters is generally not well understood at the atomistic level. We have previously shown *via* a semi-empirical thermodynamic DFT approach that the number of nitrogen vacancies on Co_3Mo_3N surfaces can be of the order of 10^{13} per cm^2 even at ambient temperature.[1] These nitrogen vacancies, due to their high concentration, could participate in catalytic reactions in competing pathways that occur on the catalyst surface and at steps. In a detailed study of the adsorption and activation of N_2 and H_2 on Co_3Mo_3N surfaces[2] with such nitrogen vacancies, we found that N_2 becomes activated at such defect sites. The effect of oxygen impurities and nitrogen vacancies on the electronic structure and surface stability of Ta_3N_5 low index surfaces has been previously investigated which showed that the former stabilise the material[3] and that the latter results in the 720 nm sub-band-gap optical absorption.[4] A rationale for the enhanced, improved photoelectrochemical activities of Ta_3N_5(110) surfaces was given based on the low dissociation barrier of water and barrier for hydrogen migration from Ta to N.[5] Although the potential development tantalum nitride based water splitting photocatalysts is well recognised, the reactivity of these materials for ammonia synthesis is acknowledged to a smaller extent. Our recent experimental reactivity screening of Co, Fe and Re doped Ta_3N_5 materials has shown a pronounced effect on the catalytic activity in Co-doped Ta_3N_5.[6] Currently, the exact role of Co in the ammonia synthesis mechanism is, however, not well understood, nor is it known whether it can participate as a promoter in surface reactions of H_2 and N_2 over Ta_3N_5. In this dispersion-corrected periodic DFT study we attempt to gain further insight about the effect that Co promoters can have on the formation of nitrogen defects (*i.e.* nitrogen vacancies) and the chemisorption of the reactants of ammonia synthesis (*i.e.* H_2, N_2) to Ta_3N_5(001), (010) and (100) surfaces.

In order to model the bulk and surfaces of Ta_3N_5 we have used the coordinates as determined by time-of-flight neutron diffraction (TOF-ND).[7] The bulk 3 × 1 × 1 unit cell of Ta_3N_5 is shown in Fig. 1a and is composed of irregular TaN_6 octahedra with both three (N^3) and four coordinate nitrogen (N^4) atoms

[a] *Kathleen Lonsdale Materials Chemistry, Department of Chemistry, University College London, 20 Gordon Street, London, WC1H 0AJ, UK. E-mail: c.r.a.catlow@ucl.ac.uk*
[b] *WestCHEM, School of Chemistry, Joseph Black Building, University of Glasgow, Glasgow G12 8QQ, UK*
[c] *School of Chemistry, Cardiff University, Park Place, Cardiff CF10 1AD, UK*

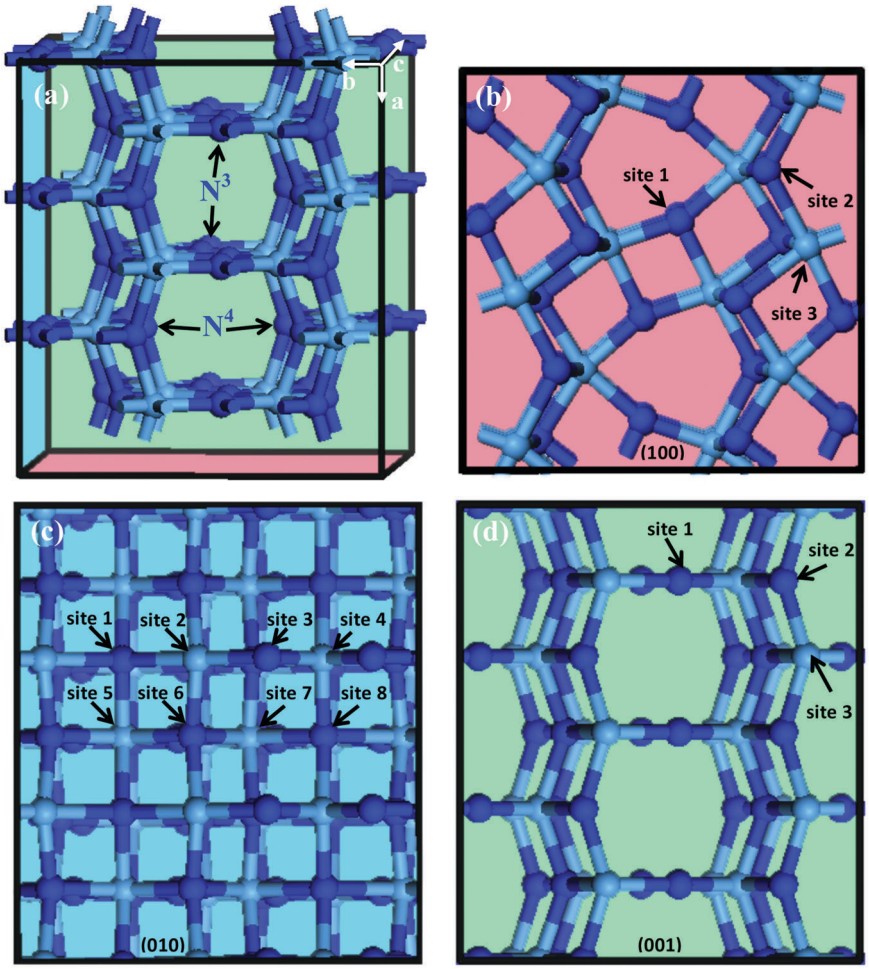

Fig. 1 (a) 3 × 1 × 1 units cell of Ta_3N_5 showing the symmetry unique nitrogen (*i.e.* N^3 and N^4 in blue) and tantalum (Ta in light blue) atoms. Low Miller index surfaces of Ta_3N_5 viewed along the crystallographic lattice vectors (b) [100] (c) [010] and (d) [001], respectively. Blue, red and green used to denote the cross section of the unit cell from which surfaces are generated. Numbers indicate symmetry unique sites where adsorption is probed.

and has the pseudo-brookite (Fe_2TiO_5) structure[8–10] shown in Fig. 1a. The 3D-framework generates channels that are 4 Å in width along the [0 0 1] lattice direction. The interstitial nitrogen was found to be labile and reactive to hydrogen that generates ammonia under reducing conditions.[6,11] The porous structure of Ta_3N_5 offers the possibility of adsorbing metal atoms to its structure. The effect of co-adsorbed cobalt atoms with respect to the adsorption of H_2 and N_2 has not been previously studied theoretically.

We have therefore calculated, *via* periodic DFT, the adsorption sites for Co atoms on Ta_3N_5. We then investigate the effect of cobalt promoters on the nitrogen vacancy formation energy on Ta_3N_5-(100), (010) and (001) surfaces. We also study the chemisorption of H_2 and N_2 on the Co promoted and plain Ta_3N_5 surfaces in order to understand the effect of Co promoters with respect to the chemisorption of the ammonia synthesis reactants.

2. Computational methods

The optimised geometry of bulk of Ta_3N_5 was modelled with 3 × 1 × 1 supercell where the corresponding 1 × 1 × 1 unit cell belongs to the space group *CmCm* (63), where a = 3.932 Å, b = 10.339 Å, c = 10.384 Å, $\alpha = \beta = \gamma = 90^\circ$. These were in good agreement with the neutron diffraction derived lattice parameters (a = 3.8862 Å, b = 10.2118 Å, c = 10.2624 Å, $\alpha = \beta = \gamma = 90^\circ$).[7] The supercell dimensions was therefore set to a = 11.795 Å, b = 10.339 Å, c = 10.384 Å, $\alpha = \beta = \gamma = 90^\circ$. The surfaces were modelled *via* slabs about 1 nm in width that had a 20 Å vacuum gap for which the surface structure is shown in Fig. 1b–d. All DFT calculations were periodic Γ-point[12] spin-polarised obtained with the use of the VASP 5.4.1 code, as Ta_3N_5 is a relatively narrow gap material, we would expect any surface dipolar effects to be compensated electronically rather than by surface reconstruction.[13,14] Exchange and correlation effects were considered within the generalized gradient approximation (GGA) using the revised Perdew–Burke–Ernzerhof (revPBE) exchange–correlation (XC) functional,[15] with the projector augmented-wave (PAW) method[16,17] used to represent core states. These were 1s to 4f for Ta, 1s for N and H, and 1s to 3p for Co. The cut-off energy for the energy of the planewaves for the bulk 3 × 1 × 1 unit cell was 800 eV, and therefore this was also used in the periodic slab calculations. Geometry optimizations were performed with a residual

force threshold on each atom of 0.01 eV Å^{-1} using the conjugate-gradient algorithm. The convergence criterion for electronic relaxation was 10^{-4} eV. The initial charge density was obtained by superposition of atomic charges. Initial adsorption configurations where such that the distance between the adsorbate and the nearest surface site was set to 2 Å in an end-on configuration for N_2 and side-on for H_2. The various adsorption sites were every symmetry unique surface site shown in Fig. 1, which resulted in 3, 8 and 3 sites for (100), (010) and (001)-surfaces, respectively. The adsorption energy was taken as the total energy difference between the fully relaxed bound state of the surface–adsorbate complex from that of the fully relaxed surface slab and the isolated molecules given by:

$$\Delta E_{\mathrm{ads,D3}} = E_{\mathrm{slab\text{-}X2}} - E_{\mathrm{slab}} - E_{\mathrm{X2}}, \quad (1)$$

where X = N, H. Dispersion corrections were included *via* the zero-damping DFT-D3 correction method of Grimme as implemented in VASP,[18] in which the following dispersion energy correction is added to the Kohn–Sham energies:

$$E_{\mathrm{disp}} = -\frac{1}{2}\sum_{i=1}^{N}\sum_{j=1}^{N}\left(s_6\frac{C_{6,ij}}{r_{ij}^{6}} + s_8\frac{C_{8,ij}}{r_{ij}^{8}}\right), \quad (2)$$

where $C_{6,ij}$ and $C_{8,ij}$ denote the averaged (isotropic) 6th and 8th order dispersion coefficients for atom pair ij and r_{ij} is the internuclear distance between atoms i and j, respectively. s_6 and s_8 are the functional-dependent scaling factors. The D3 correction was invoked in calculating the adsorption energies because it is generally known that the revPBE is unable completely to recover dispersion interactions as a result of polarisation effects of the d- and f-electrons of cobalt.

3. Results and discussion

The adsorption of N_2 and H_2 on Ta_3N_5 was studied systematically at every symmetry unique site shown in Fig. 1. We have also tested briefly whether the final configuration for an adsorption site would differ when placing the adsorbate mid-way between two symmetry unique sites but this was found to have no effect. The adsorption energies along with the relevant structural parameters of the optimised adsorbate configuration are given in Tables 1 and 2 for the (010) and (100)/(001) surface of Ta_3N_5, respectively.

3.1 N_2 adsorption on Ta_3N_5

For the adsorption of nitrogen we find that at most sites it is molecular without any activation of the N–N bond (*e.g.* Table 1 sites 1, 2, 5–8). From the dispersion-corrected adsorption energies which range between −11 to −32 kJ mol^{-1}, the adsorption of N_2 on Ta_3N_5-(010) is considered to be physisorption both to Ta and N surface atoms, with the former interaction being somewhat stronger. The larger the tilt angle, a(S–N–N) the shorter the distance, r(S–N) between N_2 and the surface. For the (010)-surface a small enhancement of the adsorption energy is observed when N_2 is adsorbed at N^4 sites compared to N^3 sites, which shows that the chemical nature of the four-coordinated and the three-coordinated nitrogen atoms differs slightly with the first having slightly more exothermic adsorption energies for molecular nitrogen.

Among the eight symmetry adsorption sites studied, two sites had a drastically different adsorption energy (Table 1, site 3 and 4) which was endothermic by 205 kJ mol^{-1}. We find that at these adsorption sites molecular nitrogen adsorbing to the surface will form an azide functional group (N_3) as shown in Scheme 1 and therefore these are in fact formation energies. The azide functional group forms on bridging surface nitrogen atoms (*i.e.* N^3). The N–N bond length of the azide in closer proximity from the surface was found to be 1.239 Å whereas the other N–N bond length was 1.146 Å, in close agreement with X-ray data of azides formed in bridging copper complexes, found to be 1.196 Å and 1.161 Å, respectively.[19] In this functional group N_2 is moderately activated based on the % bond

Table 1 Dispersion-corrected adsorption/formation energies ($\Delta E_{\mathrm{ads,D3}}$) of H_2 and N_2 adsorbed to the (010)-surface of Ta_3N_5; adsorbate bond length (r(H–H), r(N–N)), nearest surface to adsorbate separation (r(S–H), r(N–H)); adsorbate tilt angle (a(S–H–H), a(S–N–N)); adsorption site and % activation of adsorbate bond at various symmetry unique adsorption sites shown in Fig. 1c

Property	Site 1	Site 2	Site 3	Site 4	Site 5	Site 6	Site 7	Site 8	Units
Nitrogen adsorption (010)									
$\Delta E_{\mathrm{N_2,D3}}$	−22	−27	205	205	−22	−22	−14	−11	kJ mol^{-1}
r(N–N)	1.117	1.118	1.146	1.146	1.116	1.117	1.116	1.117	Å
a(S–N–N)	131.4	163.3	178.7	178.0	115.8	140.5	129.7	128.3	°
r(S–N)	3.467	2.637	1.239	1.240	3.539	3.144	3.459	3.262	Å
Type	Tilt	Tilt	End-on	End-on	Tilt	Tilt	Tilt	Tilt	
Bound to	Ta	Ta	N^3	N^3	N^4	Ta	N^3	N^3	
N_2 activation[a]	2	2	4	4	2	2	2	2	%
Hydrogen adsorption (010)									
$\Delta E_{\mathrm{H_2,D3}}$	−89	−90	−81	−175	−86	−86	−82	−82	kJ mol^{-1}
r(H–H)	0.750	0.753	0.748	2.413	0.748	0.749	0.747	0.747	Å
a(S–H–H)	88.6	87.5	165.9	n/a	128.7	105.1	138.2	124.7	°
r(S–H)	3.103	2.810	2.709	1.021	3.095	3.109	2.923	3.086	Å
Type	Side-on	Side-on	End-on	Atomic	Tilt	Tilt	Tilt	Tilt	
Bound to	N^4	Ta	N^3	N^3	N^4	N^4	N^3	N^3	
H_2 activation[b]	1	2	1	n/a	1	1	1	1	%

[a] Percent N_2 activation is defined as $[r(N_2,\mathrm{ads}) - 1.098] \times 100/1.098$. [b] Percent H_2 activation is defined as $[r(H_2,\mathrm{ads}) - 0.74] \times 100/0.74$.

Table 2 Dispersion-corrected adsorption/formation energies ($\Delta E_{ads,D3}$) of H_2 and N_2 adsorbed to the (100) and (001) surface of Ta_3N_5; adsorbate bond length (r(H–H), r(N–N)), nearest surface to adsorbate separation (r(S–H), r(N–H)); adsorbate tilt angle (a(S–H–H), a(S–N–N)); adsorption site and % activation of adsorbate bond at various symmetry unique adsorption sites shown in Fig. 1b and d, respectively

	Site 1	Site 2	Site 3	Site 1	Site 2	Site 3	
Property	Nitrogen adsorption (001)			Nitrogen adsorption (100)			Units
$\Delta E_{H_2,D3}$	−29	0	−32	−13	201	−23	kJ mol^{-1}
r(N–N)	1.123	1.113	1.118	1.112	1.158	1.116	Å
a(S–N–N)	159	92	168	152	177	174	°
r(S–N)	2.504	2.939	2.348	3.476	1.231	2.476	Å
Type	Tilt	Side-on	End-on	Tilt	End-on	End-on	
Bound to	Ta	N^4	Ta	N^4	N^4	Ta	
N_2 activation[a]	2	1	2	1	5	2	%
	Site 1	Site 2	Site 3	Site 1	Site 2	Site 3	
Property	Hydrogen adsorption (001)			Hydrogen adsorption (100)			Units
$\Delta E_{H_2,D3}$	−86	−81	−91	−85	−87	−90	kJ mol^{-1}
r(H–H)	0.752	0.749	0.7623	0.752	0.748	0.749	Å
a(S–H–H)	151	163	86	134	155	84	°
r(S–H)	2.568	2.738	2.387	2.842	2.814	3.161	Å
Type	Tilt	End-on	Side-on	Tilt	Tilt	Side-on	
Bound to	N^3	N^4	Ta	N^4	N^4	Ta	
H_2 activation[b]	2	1	3	2	1	1	%

[a] Percent N_2 activation is defined as $[r(N_2,ads) - 1.098] \times 100/1.098$. [b] Percent H_2 activation is defined as $[r(H_2,ads) - 0.74] \times 100/0.74$.

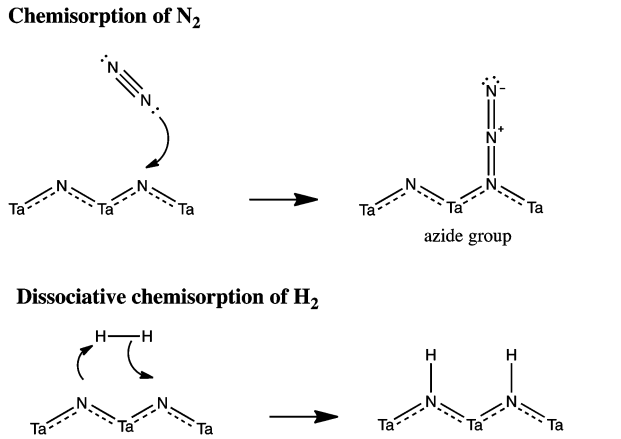

Scheme 1 Schematic showing the reactions products of N_2 and H_2 with Ta_3N_5 surfaces.

elongation which was found to be 4–5%. Based on the formation energy of the azide, this functional group appears to be quite unstable on the (010) surface of Ta_3N_5. A simplified schematic showing the adsorption site geometry of the azide group formation and the formation of >NH species due to H_2 chemisorption are shown in Scheme 1.

3.2 H_2 adsorption on Ta_3N_5

For the adsorption of H_2 we find that it is mostly molecular with only one site dissociating it and forming surface >NH groups (see Scheme 1). These >NH groups form again on bridging surface nitrogen atoms (*i.e.* N^3 sites) and their formation energy is exothermic by −175 kJ mol^{-1} for H_2 dissociating at these sites (site 4). Formation of the >NH groups can be clearly seen from structural parameters of the adsorption site shown in Table 1 for site 4. The N–H bond length is 1.021 whereas for every other adsorption site where the adsorption is molecular the N–H distance is between 2.7–3.1 Å. Furthermore this effect can be observed from the H–H distance which for the N–H groups is 2.413 Å compared to an average of 0.75 Å found for the molecularly adsorbed H_2. Based on the exothermicity of molecular H_2 adsorption, which was found between −81 to −90 kJ mol^{-1}, the adsorption here can be classified as close to chemisorption. It is very interesting to observe that although the adsorption energy of H_2 is almost −100 kJ mol^{-1} on most sites, it does not result in the dissociation of molecular hydrogen which preserves its chemical bond. Additionally, the distance at which molecular hydrogen absorbs in these configurations is quite large, ranging between 2.7 and 3.1 Å. Furthermore, we find that the adsorption energy is not very sensitive to the molecular orientation of hydrogen which adsorbs mostly in a tilt configuration but also in end-on and side-on configurations. It is interesting therefore to note how a closed shell molecule can develop such a strong interaction on Ta_3N_5-(010) surfaces even in the absence of surface metal atoms that usually have the tendency to coordinate strongly with hydrogen. Here again similarly to the adsorption of N_2, we observe a small enhancement of the adsorption energies when N_2 is adsorbed to N^4 sites compared to N^3 sites, which can be interpreted to be result of the higher polarizability of four-coordinated N atoms compared to three-coordinated N, as each Ta–N bond introduces additional polarizability due to the nature of covalent bonds observed in this semiconductor. It is interesting that based on only energetic and structural considerations the existence of the azide and NH groups can be clearly identified among the various adsorbed configurations studied.

3.3 Effect of Co-doping on nitrogen vacancy formation energies

We have investigated whether the enhanced ammonia synthesis reactivity could be attributed to the easier formation of

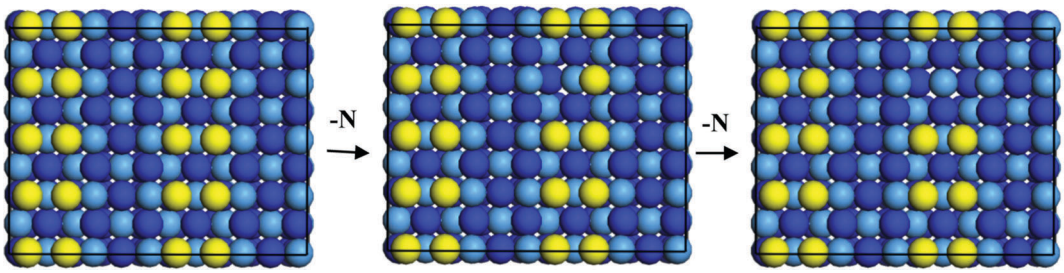

Fig. 2 Figure showing bridging nitrogen positions (yellow) on the (010) surface of Ta_3N_5 and the formation of single and double nitrogen vacancies. Surface N atoms are shown in yellow. Ta: light blue N: dark blue.

nitrogen vacancies, as these could be potential sites for nitrogen activation.[2] In particular, we have investigated the single (SVFE) and double (DVFE) vacancy formation energy of nitrogen on the (010)-surface of Ta_3N_5. Energies refer to abstraction on lattice N to form molecular nitrogen. The formation of nitrogen vacancies is schematically shown in Fig. 2 where the successive removal of a N^3 atom from the surface of Ta_3N_5-(010) is shown. The choice of single and double vacancy was such that the co-adsorbed Co could interact with both defects through nearest neighbour interactions. Other combinations of double nitrogen vacancies where the N were not in nearby positions have been omitted.

In particular, The formation of nitrogen vacancies was tested only on the (010) surface of Ta_3N_5 and the effect of cobalt dopant was examined by placing Co at two surface sites adjacent to the vacancy site (*i.e.* pos1 and pos2) and at two sub-surface sites (*i.e.* pos3 and pos4) shown in Fig. 3.

The single nitrogen vacancy formation (SVFE) energy in Ta_3N_5 is 2.89 eV, which is considerably higher than calculated for another active catalyst for ammonia synthesis, Co_3Mo_3N. There the SVFE was found to be 2.35 eV for five-coordinated nitrogen and 1.39 to 1.68 eV for three-coordinated nitrogen.[1] Therefore the surface concentration of nitrogen vacancies will be less than on Co_3Mo_3N surfaces, which, however, maybe be compensated by nitrogen vacancies at sub-surface sites, which in Ta_3N_5 may become available to the reactants due to the structure which results in 4 Å wide channels along the [001] direction as shown in Fig. 1d. We find that in Ta_3N_5 single vacancies (SV) rather than adjacent double vacancies (DV) are more stable as shown by the higher VFE in Table 3 that show that the DVFE > SVFE per vacancy by an average of 0.37 eV except at pos3, where the SV were found to be less stable than the DV. For pos4 we observe that surface and sub-surface Co co-adsorbate at nearby positions can reduce the SVFE and DVFE for nitrogen by as much as 0.94 eV. It appears that the bonding of Co at adjacent sites destabilises somewhat the Ta–N bonds, which can be attributed to the electron withdrawing nature of Co in an attempt to fill its incomplete d-shell. Therefore the effect of these Co promoters on the pronounced reactivity of the Co-doped Ta_3N_5 could be attributed to the easier formation of nitrogen vacancies in a mechanism that involves activation of nitrogen at such sites. In addition, the results tabulated in Table 3 indicate that sub-surface co-adsorption of Co results in the greatest reduction of the SVFE on Ta_3N_5, an aspect that may guide synthetic efforts generating Ta_3N_5 materials that have a large density of nitrogen vacancies, for optoelectronic applications.

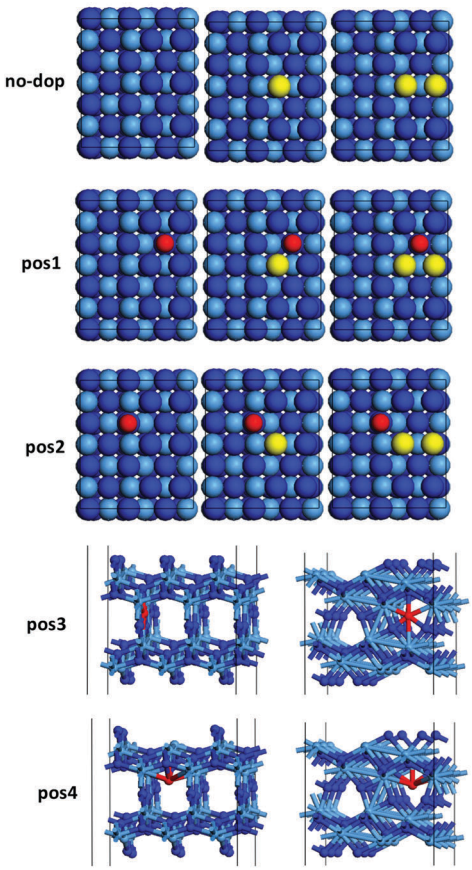

Fig. 3 (a) Top view of 3 × 1 supercell of (010) surface slab showing various doping sites for single and double N-vacancies. (b) subsurface doping sites shown along (b) [0 0 1] and (c) [1 0 0], directions.

Table 3 Summary of single (SVFE) and double (DVFE) nitrogen vacancy formation energies for Co-doped (010) surfaces of Ta_3N_5. Energies are given per vacancy

	SVFE (eV)	DVFE (eV)
No-dop	2.89	3.16
pos1	2.52	2.66
pos2	2.32	2.78
pos3	2.72	2.38
pos4	1.95	2.57

Table 4 Table that summarises the adsorption energy of Co at various sites on Ta_3N_5-(001), (010) and (001) surfaces

Site	ΔE_{ads} (kJ mol^{-1})	Structure	Co–N bonds	Site	ΔE_{ads} (kJ mol^{-1})	Structure	Co–N bonds
Ta_3N_5-(010)				Ta_3N_5-(001)			
1	−200		1	1	−361	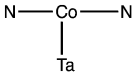	2
2	−266		1	2	−227		1
3	−206		1	3	−252	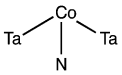	1
4	−376	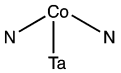	2	Ta_3N_5-(100)			
5	−302	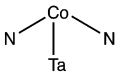	2	1	−397	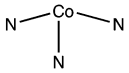	3
6	−398	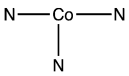	3	2	−320	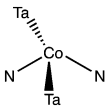	2
7	−389	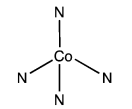	4	3	−151		0
8	−373	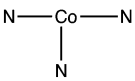	3				

3.4 Effect of Co promoters on H_2 chemisorption

We have further studied the adsorption of cobalt at various sites on the surface of Ta_3N_5 in order to understand its bonding and locate the energetically lowest doping sites. These results are tabulated in Table 4.

We find that cobalt generally adsorbs more strongly when it is coordinated to surface nitrogen atoms rather than surface tantalum atoms, which can be clearly seen by the adsorption studies of Co atoms at the various symmetry unique adsorption sites of Ta_3N_5. We have studied the adsorption of Co at the sites shown in Fig. 1. Although the adsorption structure of Co at each site has its own distinct stereochemical structure, we observed a trend of the adsorption energy as a function of the number of nitrogen atoms with which cobalt is coordinated. In particular, we found that the weakest adsorption of cobalt occurs when it interacts with a single surface tantalum atom (100-site 3) where the adsorption energy is −151 kJ mol^{-1}, which is more than 50 kJ mol^{-1} lower than the adsorption energy of Co when it interacts only with a nitrogen atom (010-site 1) which ranges between −200 to −266 kJ mol^{-1}. The adsorption energy of Co with two surface nitrogen atoms is in the range of −301 to −376 kJ mol^{-1}. Lastly the adsorption energy of Co with 3 or 4 surface nitrogen atoms is in the range −373 to −397 kJ mol^{-1}. These results show that the attachment of Co to nitrogen is more energetically favourable and depends on the number of Co–N bonds formed. In particular we find that Co will adsorb more favourably at sites that are nitrogen rich and where the nitrogen can complex with cobalt in a square planar configuration where one ligand is missing (*e.g.* 010-site 8 and 010-site 5). The average Co–N bond length was found to be 1.86 Å in close agreement with the sum of the covalent radius of values N: 71 pm and Co: 126 pm which is 1.96 Å.[20] Based on the sphere-in-contact model this result suggests the formation of covalent bonds between nitrogen and cobalt.[21] However, the electronic structure of Ta_3N_5 does not have any unpaired electrons on the surface nitrogen, which indicates when cobalt is co-adsorbed, these sites are re-hybridized into states with unpaired electrons, that can then form the covalent Co–N.

We next study how Co promoters affect the chemisorption of H_2. Here we have again studied the adsorption of a single H_2 molecule in a side-on configuration at each site depicted in Fig. 1.

The adsorption of H_2 on Ta_3N_5 is mainly molecular with adsorption energies in a narrow range (*i.e.* −81 to −90 kJ mol^{-1}) apart from one site on the (010)-surface which is shown by a white arrow in Fig. 4. At this site is chemisorbs dissociatively to form surface >NH species. Upon addition of cobalt to the surface of Ta_3N_5 at the various adsorption sites depicted in Fig. 1, we observe that the chemisorption of H_2 changes drastically with more sites promoting the dissociation of molecular hydrogen in the form of atomically chemisorbed –H species. Based on the average length of the Co–H bond, we find that it is in close agreement with the sum of the covalent radius of Co and H and therefore indicates covalent bonding of H with cobalt. Additionally for every site the adsorption energy becomes more

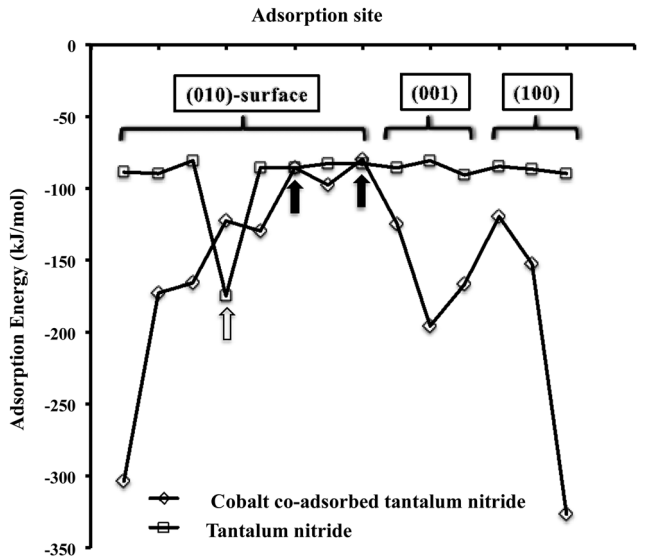

Fig. 4 Graph showing the dispersion-corrected adsorption energy of H_2 on plain and Co-doped Ta_3N_5-(001), (010) and (001) surfaces.

exothermic apart from two sites shown by the black arrows in Fig. 4, where the adsorption remains molecular. At both these sites Co is coordinated to 3 nitrogen atoms and therefore does not dissociatively chemisorb H_2, but only adsorbs it in a side-on configuration. This result clearly suggests that co-adsorbed cobalt atoms on the various surfaces of Ta_3N_5 will promote the formation of –H species which could be active intermediates in the hydrogenation of surface nitrogen in surface reactions mechanism of the Langmuir–Hinshelwood type, where both –N and –H originates from surface adsorbates.

4. Conclusions

In this periodic DFT study we studied systematically the adsorption of the reactants of ammonia synthesis (*i.e.* H_2 and N_2) on Ta_3N_5 and have found potential reaction intermediates relevant to the ammonia synthesis reaction and have explained the effect of Co promoters. The adsorption of nitrogen was found to be mostly molecular and non-activated with side-on, end-on and tilt configurations. At bridging nitrogen sites (Ta–N–Ta) it results in an azide functional group formation with a formation energy of 205 kJ mol^{-1}. H_2 was found to also chemisorb molecularly with an adsorption energy in the range −81 to −91 kJ mol^{-1}. At bridging nitrogen sites it adsorbs dissociatively forming >NH groups with an exothermic formation energy of −175 kJ mol^{-1} per H_2. Co-adsorption of cobalt was found to occur mostly at the nitrogen rich sites of the surface, with an adsorption energy that ranged between −200 to −400 kJ mol^{-1}. We have shown how cobalt can lower the vacancy formation energy for nitrogen in Ta_3N_5 and become active centres for dissociative hydrogen chemisorption.

Acknowledgements

This study was supported by EPSRC funding (EP/L026317/1, EP/L02537X/1). *Via* our membership of the UK's HEC Materials Chemistry Consortium, which is funded by EPSRC (EP/L000202/1), this work used the ARCHER UK National Supercomputing Service (http://www.archer.ac.uk).

References

1 C. D. Zeinalipour-Yazdi, J. S. J. Hargreaves. and C. R. A. Catlow, *J. Phys. Chem. C*, 2015, **119**, 28368.
2 C. D. Zeinalipour-Yazdi, J. S. J. Hargreaves and C. R. A. Catlow, *J. Phys. Chem. C*, 2016, **120**, 21390.
3 J. Wang, A. Ma, Z. Li, J. Jiang, J. Feng and Z. Zou, *Phys. Chem. Chem. Phys.*, 2015, **17**, 23265.
4 J. Wang, A. Ma, Z. Li, J. Jiang, J. Feng and Z. Zou, *Phys. Chem. Chem. Phys.*, 2015, **17**, 8166.
5 J. Wang, A. Ma, Z. Li, J. Jiang, J. Feng and Z. Zou, *Phys. Chem. Chem. Phys.*, 2016, **18**, 7938.
6 S. Laassiri, C. D. Zeinalipour-Yazdi, C. R. A. Catlow and J. S. J. Hargreaves, *Catal. Today*, 2017, **286**, 147.
7 N. E. Brese, M. O'Keeffe, P. Rauch and F. J. DiSalvo, *Acta Crystallogr., Sect. C: Cryst. Struct. Commun.*, 1991, **47**, 2291.
8 S. J. Henderson and A. L. Hector, *J. Solid State Chem.*, 2006, **179**, 3518.
9 N. E. Brese, M. O'Keeffe, P. Rauch and F. J. DiSalvo, *Acta Crystallogr., Sect. C: Cryst. Struct. Commun.*, 1991, **47**, 2291.
10 J. Strähle, *Z. Anorg. Allg. Chem.*, 1974, **402**, 47.
11 A. M. Alexander, J. S. J. Hargreaves and C. Mitchell, *Top. Catal.*, 2012, **55**, 1046.
12 H. J. Monkhorst and J. D. Pack, *Phys. Rev. B: Solid State*, 1976, **13**, 5188.
13 G. Kresse and J. Furthmüller, *Phys. Rev. B: Condens. Matter Mater. Phys.*, 1996, **54**, 11169–11186.
14 G. Kresse and J. Hafner, *Phys. Rev. B: Condens. Matter Mater. Phys.*, 1993, **47**, 558.
15 J. P. Perdew, K. Burke and M. Ernzerhof, *Phys. Rev. Lett.*, 1996, **77**, 3865.
16 G. Kresse and D. Jouber, *Phys. Rev. B: Condens. Matter Mater. Phys.*, 1999, **59**, 1758–1775.
17 P. E. Blöchl, *Phys. Rev. B: Condens. Matter Mater. Phys.*, 1994, **50**, 17953.
18 S. Grimme, J. Antony, S. Ehrlich and H. Krieg, *J. Chem. Phys.*, 2010, **132**, 154104.
19 K. Matsumoto, S. I. Ooi, K. Nakatsuka, W. Mori, S. Suzuki, A. Nakahara and Y. Nakao, *J. Chem. Soc., Dalton Trans.*, 1985, 2095.
20 B. Cordero, V. Gómez, A. E. Platero-Prats, M. Revés, J. Echeverría, E. Cremades, F. Barragán and S. Alvarez, *Dalton Trans.*, 2008, 2832.
21 C. D. Zeinalipour-Yazdi, D. P. Pullman and C. R. A. Catlow, *J. Mol. Model.*, 2016, **22**, 40.